Open-Source Body-Powered Prosthesis with a Selective Gear-Based Clutch Mechanism for Switching Grasp Types

Evan Pacic, Remi Jones, Elijah Paiz, and George P. Kontoudis

***Abstract*— Body-powered prosthetic hands remain widely used due to their mechanical simplicity, durability, low-cost, and intuitive cable-driven control. However, most existing body-powered systems are limited to a single grasp pattern, restricting grasping capabilities. Although underactuated and compliant mechanisms have improved grasp adaptability, expanding functionality—without introducing electronics, servomotors, or pumps—remains a fundamental challenge. This paper introduces a selective gear-based clutch mechanism that enables a single body-powered input to actuate multiple grasp types of an underactuated prosthetic hand. The mechanism operates by translating a sliding gear into discrete engagement positions, mechanically routing the input tendon to different output pathways. This architecture enables four functional modes for the user: (i) flexion/extension (F/E) of all fingers; (ii) adduction/abduction (Ad/Ab) of four fingers; (iii) thumb opposition; and (iv) a neutral rest mode, all actuated by a single input cable. The highly underactuated hand incorporates two parallel whiffletree differentials to distribute forces across fingers. The body-powered system is evaluated through bench testing and functional assessment using the Brief Activity Measure for Upper Limb Amputees (BAM-ULA). Experimental results demonstrate consistent force transmission. The results indicate that the proposed mechanism extends functionality while preserving affordability.**

I. Introduction

Body-powered prosthetic hands are widely adopted due to their mechanical robustness, low maintenance, intuitive feedback, and significantly lower cost compared to their myoelectric counterparts [1], [2]. However, most designs support only a single grasp pattern, limiting functionality for diverse activities of daily living [3], [4]. While underactuated mechanisms and compliant structures have improved grasp adaptability [5], they do not inherently enable switching between fundamentally different grasp types. Differential mechanisms, particularly whiffletrees, effectively distribute forces among fingers using a single actuator [6]–[9], achieving affordable dexterity with actuator-to-finger ratios below unity [10], [11]. Mechanically reconfiguring prosthetic hands to access multiple functional modes without actuators or multiple input cables remains challenging.

Related Work: Prosthetic hands actuated with many motors offer robust solutions but are often expensive, heavy, and susceptible to mechanical and environmental failure [12]. In contrast, body-powered prostheses are lightweight, durable, and affordable, yet they sacrifice dexterity and grasp versatility, limiting the user's ability to perform complex daily tasks [13], [14]. Body-powered prostheses have evolved with improvements in durability, weight reduction, and actuation efficiency [1]. In [15], the authors achieved over 95% transmission efficiency through rolling links, requiring 3–$4\,\mathrm{N}$ operating force with glove compensation. Variable transmission systems can potentially optimize the relationship between user input and grip forces as well as enable handling of wider object varieties with reduced shoulder motion [16]. In [17], the authors demonstrated potential for reducing shoulder exertion through continuously varying transmission.

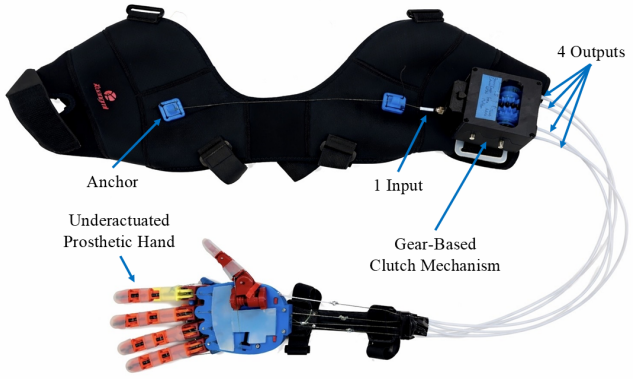

Fig. 1. The proposed anthropomorphic prosthetic hand integrates underactuated finger mechanisms with a body-powered actuation system. The design incorporates a gear-based selective clutch mechanism for mechanically switching between functional modes and internal differential mechanisms for compliant force distribution.

Underactuated designs leverage mechanical intelligence for adaptive grasping with fewer actuators than degrees of freedom [3], [18]. In [19], the authors introduced a mechanically programmable gripper with lever-based differential for force distribution. The authors in [20] achieved mean errors below 4% between theoretical predictions and experimental grasping forces through kinetostatic analysis. Optimized transmission efficiency using spherical four-bar mechanisms is shown to increase workspace by 3.5 times [21]. In this work, the tendon-driven body-powered system is connected to a highly underactuated prosthetic hand using two parallel whiffletree differential mechanisms.

Prosthetic hands are often equipped with selectively lockable and mode-switching mechanisms [9]. In [7], the authors introduced a selectively lockable mechanism to manually block the motion of fingers. This mechanism was later automated by a low-torque actuator [8] and combined with

This work was supported by the First-year Innovation & Research Scholar Training (FIRST), Mines Undergraduate Research Fellowship (MURF), and Summer Undergraduate Research Fellowship (SURF) of the Office of Undergraduate Research, Colorado School of Mines.

All authors are with the Mechanical Engineering Department, Colorado School of Mines, Golden, CO, USA. {evan_pacic, rjones1, paiz, george.kontoudis}@ mines.edu.

a body-powered prosthesis [22]. A ratcheting mechanism for automatic finger locking, showing higher success for lightweight objects and cylindrical shapes was introduced in [23]. However, existing body-powered hands lack a single-input multi-output mechanism for switching between different functional modes, which this work addresses.

Human hand synergies show that two principal components account for at least 80% of grasping [24], inspiring synergy-based designs [10]. In addition, [25] found that affordable tendon-driven hands achieved 48–57% of human performance, with two principal components explaining over 80% of tendon displacement variance. Manipulation synergies [26] as well as postural synergies during environmental constraint exploitation [27] inspired the design of highly underactuated anthropomorphic robot hands with manipulation skills [28]–[30]. Postural synergies are employed in the design process of this work to identify the output functional modes of the prosthetic hand.

We propose a selective gear-based clutch mechanism that enables a single body-powered input to actuate multiple functional modes in an underactuated prosthetic hand (Fig. 1). The mechanism employs a sliding selector that translates a compact input gear into discrete engagement positions, each coupling the input tendon to a distinct gear train while mechanically locking the remaining outputs through fixed sector gears. Integrated into a lightweight, underactuated anthropomorphic hand with parallel whiffletree differentials, this architecture provides four functional modes: all-finger flexion/extension, four-finger adduction/abduction, thumb opposition, and a neutral rest mode. The system is experimentally validated through standardized functional assessment (BAMULA), thumb opposition testing (Kapandji), and quantitative grasp force measurements, demonstrating functionality with consistent force transmission. Beyond prosthetics, the proposed design contributes a mechanically reconfigurable single-input multi-output transmission mechanism for underactuated robotic hands, offering a passive alternative to motorized reconfiguration while preserving simplicity.

Contribution: First, we introduce a selective gear-based clutch mechanism that enables multiple functional outputs from a single body-powered input. The mechanism mechanically routes tendon actuation through a shifting gearbox that selectively engages distinct transmission pathways while locking inactive outputs, enabling switching between grasp types without unintended back-driving. Second, we introduce an open-source, lightweight, and low-cost body-powered prosthetic system that integrates the proposed clutch mechanism and a prosthetic hand with parallel whiffletrees for adaptive force distribution. The system demonstrates robust grasping across a wide range of daily tasks while preserving simplicity and accessibility.

II. System Design and Analysis

In this section, we present the design of the body-powered system. We show the structure of the fingers, discuss the prosthetic hand design, and introduce the selective gear-based clutch mechanism along with a force transmission analysis.

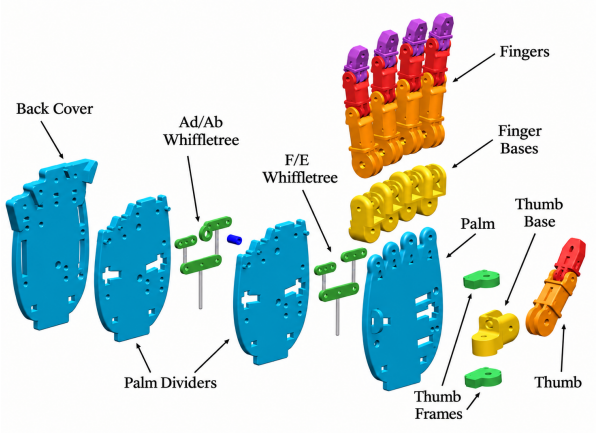

Fig. 2. Exploded view of underactuated hand mechanism. The hand consists of: i) four fingers with three pin joints each and springs for passive extension, ii) a thumb with two pin joints and springs for passive extension, iii) a thumb base and frames that enable the rotation, iv) the whiffletree controlling flexion/extension of all fingers, v) the whiffletree controlling adduction/abduction of the four fingers, and vi) the remaining components that make up the hand body and the palm.

A. Finger Structure

The finger structure follows a bio-inspired tendon-driven architecture in which cables actuate the joints. The finger design is adapted from [31], with modifications introduced to support additional lateral motion at the metacarpophalangeal (MCP) joint. Each of the four fingers[1] consists of proximal, middle, and distal phalanges, while the thumb includes proximal and distal segments, as shown in Fig. 2. The fingers use exclusively pin joints with passive elastic elements (i.e., springs) to return to their neutral configuration. All fingers are attached to the palm with a modular bolt-nut interface that allows individual fingers to be easily assembled or replaced.

The geometric proportions of the fingers were selected according to anthropometric models of the human hand [32]. In particular, segment lengths and joint locations were derived from statistical anthropometric studies based on radiography, which relate finger segment dimensions to overall hand size.

B. Prosthetic Hand Design

The prosthetic hand employs a tendon-driven actuation architecture consisting of three tendon-routing systems with two whiffletrees (Fig. 2). Similarly to the finger structure, the geometric characteristics of the palm and the placement of the fingers are determined by anthropometric models [32].

The first tendon-routing system generates flexion/extension (F/E) for all fingers. Tendon forces are distributed across the four fingers using a whiffletree mechanism. This whiffletree also drives the thumb F/E through the central lever. In contrast to [33], thumb flexion is mechanically coupled with this system, allowing simultaneous flexion of all fingers using a single tendon input. The second tendon-routing system controls adduction/abduction (Ad/Ab) of the four fingers at the MCP joints. Similar to the flexion mechanism, tendon

[1]The index, middle, ring, and pinky are termed as four fingers.

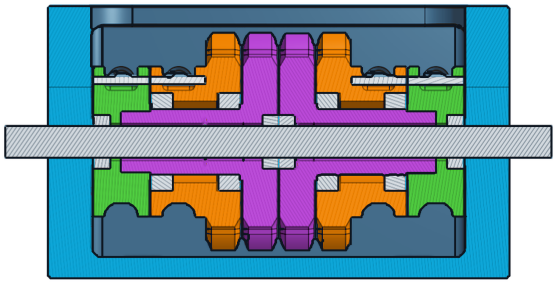

Fig. 3. Cross-sectional view of the gear-based clutch mechanism showing from left to right: Four finger Ad/Ab pulley (green), all finger F/E Gear and pulley (orange), four finger Ad/Ab gear (purple), neutral gear (purple), thumb opposition gear and pulley (orange), and neutral pulley (green).

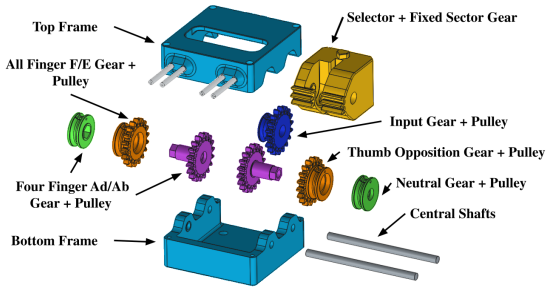

Fig. 4. Exploded view of the mode-switching transmission illustrating the top and bottom frames, selector with fixed sector gear, input gear–pulley assembly, output gear–pulley assemblies, and central shafts. The four finger Ad/Ab gear (left purple) and pulley (left green) are interconnected. Similarly, the neutral gear (right purple) and pulley (right green) are interconnected. The all finger F/E gear and pulley (left orange) and the thumb opposition gear and pulley (right orange) are designed as single parts. The input gear and pulley (blue) is inserted into the selector (yellow).

forces are distributed through a whiffletree. To maintain a stable reference configuration, the Ad/Ab differential branch corresponding to the middle finger is mechanically blocked, allowing lateral motion only for the index, ring, and pinky fingers. This arrangement enables finger spreading, while preserving structural symmetry of the hand. The third tendon-routing system actuates thumb opposition, enabling continuous lateral motion of the thumb.

Lever-based whiffletree differentials are used because they provide a simple, lightweight, and reliable means of distributing tendon forces while preserving passive adaptability. This design enables coordinated finger motion and adaptive force sharing across fingers while maintaining the mechanical simplicity required for body-powered prosthetics. Note that the thumb is actuated through two tendon-routing systems, one dedicated to flexion and another to opposition, reflecting its central role in grasping [34], [35].

C. Gear-Based Clutch Mechanism

The proposed mode-switching transmission enables selective coupling between a single body-powered input cable and one output of several, while simultaneously constraining the remaining outputs. The mechanism is a compact gear-based clutch that allows the user to switch between multiple functional modes without introducing additional actuators.

In Fig. 3, we illustrate a cross-sectional view of the mechanism and Fig. 4 presents the exploded view of the main components. The transmission is composed of a top frame, bottom frame, central shafts, a selector with integrated fixed sector gear, an input gear and pulley, and four output gear/pulley assemblies corresponding to the different functional modes. These output assemblies include the F/E gear and pulley for flexion/extension of all fingers, the finger Ad/Ab gear and pulley for lateral motion of the four fingers, the thumb opposition gear and pulley for thumb opposition, and a neutral gear and pulley for the rest configuration.

The mechanism also supports a reset-to-rest operation for each functional mode. To return the mechanism to its rest configuration, the user releases the input cable while the corresponding mode is engaged, allowing the passive extension springs to restore the fingers to their open position. Since each tendon is isolated by the clutch mechanism, resetting multiple modes requires sequentially engaging each mode and releasing the cable to allow the springs to return the tendons to their rest positions.

Functional mode selection is achieved through the selector, which houses the fixed sector gear and allows axial translation of the input gear along the central shaft. By sliding the selector, the input gear is aligned with one of the output gears. In every configuration, the input gear meshes with one selected gear, while the remaining output gears engage the fixed sector gear. Because the sector gear is stationary relative to the frame, the non-selected gears are constrained and their corresponding tendon pathways remain fixed. This ensures that motion is only transmitted to the corresponding tendon routing system, while the rest functional modes remain in their previous configuration, preventing back-driving.

The cross-sectional view in Fig. 3 shows the assembled mechanism and illustrates how the gears interact inside the housing formed by the top and bottom frames. The central shafts (gray) support the gear/pulley assemblies and ensure proper alignment of the transmission components. Needle bearings (gray) integrated into the selector and input gear allow smooth axial translation during mode switching while minimizing friction during rotation. The exploded view in Fig. 4 highlights the compact arrangement of the four output gear/pulley assemblies along the central shafts. Each output gear is coupled with its pulley so that rotational motion of the gear directly produces tendon displacement. The pulleys guide the corresponding cables for each functional mode, including all finger F/E, four finger Ad/Ab, and thumb opposition. The neutral gear/pulley assembly serves to maintain cable tension and stabilize the mechanism when no actuation mode is engaged.

The assembly forms a gearbox mechanism that enables functional mode switching. By mechanically constraining inactive outputs, the input drives only the selected gear train. This architecture provides a purely mechanical solution for multiple grasp types in body-powered prosthetic hands.

D. Gear Mechanism Analysis

Once a gear train is engaged, the relationship between the angular displacement of the input gear and the selected output gear is determined by the gear ratio $\theta_{\text{out},i} = G_i\theta_{\text{in}}$, where θ_{in} is the angular displacement of the input gear, $\theta_{\text{out},i}$ the angular displacement of the output gear $i = 1, \ldots, 4$, and G_i the gear ratio. The gear ratio is given by $G_i = N_{\text{in}}/N_{\text{out},i}$, where N_{in} is the number of teeth of the input gear and $N_{\text{out},i}$ of the selected output gear. The rotation of the output gear produces tendon displacement $\delta_i = r_i\theta_{\text{out},i}$ through the output pulley of radius r_i. For a body-powered input cable with displacement ΔL_{in} applied to an input pulley of radius R_{in}, the input gear rotation is $\theta_{\text{in}} = \Delta L_{\text{in}}/R_{\text{in}}$. Combining these relationships yields the overall kinematic transmission ratio of the i-th gear,

$$K_i = \frac{\delta_i}{\Delta L_{\text{in}}} = \frac{G_i r_i}{R_{\text{in}}}, \tag{1}$$

which determines how the motion of gear i is converted into tendon displacement.

Assuming ideal gear transmission, the torque relationship between input and output gears is $\tau_{\text{out},i} = \tau_{\text{in}}/G_i$. If the body-powered cable applies an input force F_{in}, the input torque is $\tau_{\text{in}} = F_{\text{in}}R_{\text{in}}$. The resulting output tendon force becomes,

$$F_{\text{out},i} = \frac{\tau_{\text{out},i}}{r_i} = \frac{R_{\text{in}}}{G_i r_i}F_{\text{in}}.$$

Thus, the transmission ratio of functional mode i yields,

$$\Gamma_i = \frac{F_{\text{out},i}}{F_{\text{in}}} = \frac{R_{\text{in}}}{G_i r_i}. \tag{2}$$

Note that the kinematic transmission of tendon displacement (1) and the force amplification (2) are strictly reciprocal $\Gamma_i = 1/K_i$ in the lossless case, which reveals a fundamental design trade-off. Increasing the gear ratio G_i or the output pulley radius r_i, or reducing the input pulley radius R_{in}, increases the available tendon displacement at the cost of reduced force amplification. Sufficient tendon stroke is required to fully flex the underactuated fingers, so these parameters must be selected to satisfy the stroke requirement of the hand while maximizing the transmitted tendon force.

Practical operation introduces losses due to gear contact, bearing friction, and tendon routing friction. The overall efficiency of the transmission can be approximated as the product $\eta_i \approx \eta_{\text{gear}}\eta_{\text{bearing}}\eta_{\text{tendon}}$. The effective output tendon force for gear i becomes,

$$F_{\text{out},i}^{\text{actual}} = \eta_i \, \Gamma_i \, F_{in}.$$

Note that using typical values for small mechanical transmissions ($\eta_{\text{gear}} \approx 0.96$, $\eta_{\text{bearing}} \approx 0.98$, and $\eta_{\text{tendon}} \approx 0.92$) [36], the overall efficiency is approximately $\eta_i \approx 0.87$.

Output tendons connect to the F/E whiffletree distributing force among all fingers $F_{\text{out},i} = \sum_{j=1}^{5} F_j$. Thus, when a finger contacts an object, the corresponding lever rotates and the remaining fingers continue to flex, enabling shape adaptation during grasping with a fixed force ratio.

TABLE I
MECHANICAL CHARACTERISTICS OF THE BODY-POWERED PROSTHESIS

Actuation input	Single body-powered cable
Functional modes	4
Transmission mechanism	Gear-based clutch
Differential mechanisms	2 whiffletrees
Structural materials	PLA, PETG
Contact material	Cast silicone elastomer
Total hardware cost	\$138
Weight (hand)	331 g
Input Pulley Radius (R_{in})	9.25 mm
Output Pulley Radius (r_i)	11.25 mm
Gear Ratio (G_i)	1.0
Four Finger Spring Stiffness	0.152 N/mm
Thumb Spring Stiffness	0.657 N/mm

III. FABRICATION PROCESS

In this section, we describe the fabrication of the proposed body-powered prosthetic system which is comprised of the underactuated, anthropomorphic hand, gear-based clutch mechanism, tendon-routing systems (i.e., one input and four outputs), and the back-harness. All custom parts are either FDM 3D printed from PLA or PETG, and cast elastomer made with 3D printed molds. All non-printed parts and metal components, including shafts, pins, fasteners, and needle roller bearings, are commercially available off-the-shelf (COTS). In Table I, we summarize the primary characteristics and variables of the body-powered prosthetic system. We select the gear ratio to be $G_i = 1.0$ for all gears i. Thus, the transmission ratio (2) results in $\Gamma_i = 0.82$ (or $\Gamma_i \approx 0.72$ including losses) for all gears i, trading transmission force over stroke. This value was chosen to provide equal tendon stroke across modes and to keep the clutch compact. Since each mode has a corresponding gear pair, G_i could be different for every mode (e.g., favoring force in F/E and stroke in Ad/Ab), but we leave this for future work. Excluding 3D printing filament and silicone material costs, the total hardware cost of the prosthetic system is \$138. The reliance on 3D printing with COTS materials reduces costs and increases the wider approachability of this project. The prosthetic hand weighs $331\,\text{g}$, below both the $400\,\text{g}$ average mass of the human hand, and the $400\,\text{g}$ and $500\,\text{g}$ weight specifications proposed for adult prosthetic hands [3]. To promote reproducibility and open-source development [37], all CAD files are available at the GitHub repository[2].

A. Hand Fabrication

The prosthetic hand is composed primarily of 3D printed components. Structural components of the gear-based clutch mechanism and pulley assemblies are fabricated using PETG due to its improved ductility and impact resistance. Each of the four fingers consists of three phalangeal segments connected through stainless-steel pin joints, while the thumb

[2]https://github.com/mpala-lab/BodyPowered-MultiMode-Prosthetic-Hand

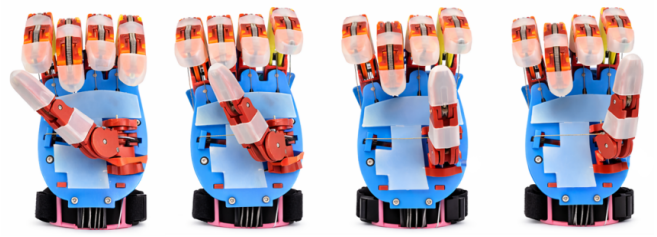

Fig. 5. Hand performing the Kapandji Test: touching the thumb to the tip of each of the four fingers.

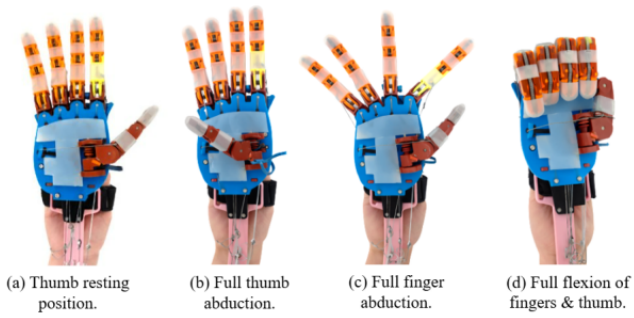

Fig. 6. Hand postures of the proposed prosthesis, including (a) neutral resting configuration, (b) full thumb opposition, (c) full finger abduction, and (d) full flexion of the fingers and thumb.

Fig. 7. Range of motion of the thumb with continuous opposition.

includes two segments. We selected pin joints to allow flexion and extension while maintaining mechanical robustness. Passive extension springs are mounted along the dorsal side of the fingers to restore the hand to an open configuration when tendon tension is released [31]. The finger modules are attached to the palm through a modular bolted interface. Finger pads are fabricated using hybrid deposition manufacturing [38] (SmoothOn Dragonskin 20) to increase friction at the contact surfaces and improve grasp stability.

B. Anthropomorphic Spring Calibration

Anthropomorphic principles were considered during the fabrication of the prosthetic hand to ensure that the resulting kinematic behavior and restoring forces approximate those of the human hand [39]. In addition to geometric proportions (Section II-A, Section II-B), springs are selected to approximate the motion of human fingers during flexion. The stiffness of the extension springs was determined experimentally using the Kapandji thumb opposition test, a widely used clinical test for evaluating human hand function after surgeries [40]. The Kapandji test quantifies thumb opposition ability based on the thumb tip reaching specific locations across the palm and opposing fingers. During the fabrication process, the spring stiffness values were iteratively adjusted so that the prosthetic thumb could reach the same positions defined by the Kapandji test as shown in Fig. 5.

C. Tendon-Driven Actuation and Back Harness Interface

The prosthetic hand is actuated through several tendon-routing systems that combine Bowden cable transmission with a body-powered back harness. The harness converts forward shoulder rotation into cable displacement, which is transmitted to the prosthetic hand through low-friction Bowden cables. One end of the input cable is anchored near the shoulder region, while the opposite end connects to the input pulley of the gear-based clutch mechanism (Fig 1). Flexion of the shoulders increases the cable excursion, producing displacement of the input tendon that drives the internal transmission system. Depending on the selected functional mode, the motion is routed to the corresponding tendon pathway within the hand.

Three primary tendon-routing systems are implemented within the prosthetic hand: (i) flexion/extension (F/E) of all fingers, (ii) adduction/abduction (Ad/Ab) of the four fingers, and (iii) thumb opposition. Two internal whiffletree differentials distribute forces across the fingers during F/E and Ad/Ab, enabling adaptive grasping and coordinated motion. Bowden cable routing allows flexible placement of the harness relative to the hand.

IV. Experiments and Results

A. Experimental Setup

To evaluate the capabilities of the proposed body-powered prosthetic system, we conduct a series of experiments including gesture postures, thumb opposition, standardized functional assessment, grasp demonstrations with everyday objects, and quantitative grasp force measurements. Functional performance is assessed using the Brief Activity performance Measure for Upper Limb Amputees (BAM-ULA) [41]. The BAM-ULA is a performance-based protocol consisting of ten unilateral tasks representative of activities of daily living, including object grasping and manipulation, lifting, and tool use. In addition to the BAM-ULA assessment, hand gestures and thumb opposition capability are evaluated. Experiments were performed by one able-bodied participant, with the prosthesis worn alongside the intact limb. The participant had no prior prosthesis experience.

B. Hand Postures and Thumb Opposition

The range of hand postures is evaluated to examine the versatility of the prosthetic hand and illustrate how the different functional modes enable a variety of grasp types. In Fig. 6, we show a subset of hand postures, including the rest configuration, full thumb opposition, full finger abduction, and full flexion of the fingers and thumb. The combination of

TABLE II
BAM-ULA PERFORMANCE RESULTS

Test	Task Description	Score (/10)	Success (%)
1	Tuck shirt into back of pants	10	100
2	Place 20 lb bag on shelf	10	100
3	Open sealed water bottle and drink	0	0
4	Remove wallet from pocket*	0	0
5	Insert wallet into pocket*	10	100
6	Remove 1-gallon jug from refrigerator	10	100
7	Open gallon jug and pour	8	80
8	Brush/comb hair	10	100
9	Use a fork	7	70
10	Open door (latch handle)**	10	100

Side pocket used instead of back pocket.

***Latch handle used instead of round doorknob.*

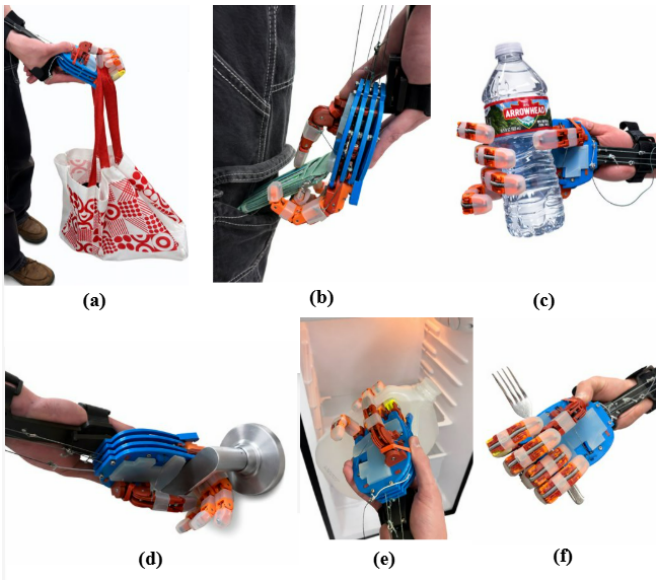

Fig. 8. Task execution of the BAM-ULA test using the body-powered prosthesis: (a) lifting a 20 lb bag (Task 2); (b) Placing a wallet into a pocket (Task 5); (c) Manipulating a sealed water bottle (Task 3); (d) Turning a door handle (Task 10); (e) Removing a 1-gallon jug from a refrigerator (Task 6); and (f) Grasping a fork (Task 9).

F/E, Ad/Ab, and thumb opposition allows the hand to adapt its configuration to objects of different sizes and shapes, supporting power grasps, precision grasps, and intermediate grasp types [42].

The thumb plays a critical role in establishing effective opposition during grasping. In Fig. 7, we illustrate the thumb range of motion. Unlike many prosthetic designs that rely on discrete thumb positions or manually repositioned thumb modules [7], [8], the proposed mechanism provides a continuous range of thumb motion through the thumb opposition tendon-routing system. Thus, the continuous thumb motion facilitates transitions between different grasp types without requiring manual reconfiguration. By adjusting the thumb position, the user can achieve both lateral pinch configurations and more enveloping grasp postures for various object shapes and sizes.

C. BAM-ULA Task Performance

Each task is repeated 10 times to evaluate repeatability and consistency of execution. A successful completion counted as one point per trial, yielding a maximum score of 10 per task and 100 total possible points. All tasks are performed using the prosthetic hand side unless environmental constraints require minor modifications. In Table II, we list the quantitative performance across all BAM-ULA tasks and in Fig. 8 we show some executions of the BAM-ULA tasks using the proposed body-powered prosthesis. The prosthetic system achieves an overall score of $75/100$, corresponding to a 75% aggregate task completion rate across 100 repeated trials. Several tasks of the BAM-ULA test are modified: (i) Side pocket used instead of back pocket (Tests 4 and 5); (ii) Mini refrigerator requiring crouching (Test 6); and (iii) Latch handle substituted for round doorknob (Test 10). The latch handle likely reduces torsional precision requirements relative to a round doorknob, potentially elevating performance in Test 10. Conversely, crouching to access the mini refrigerator increases ergonomic complexity in Test 6.

High success rates are observed in tasks that require grasping, lifting, object transport, and hand-arm manipulation, such as tucking a shirt (Task 1), placing a 20 lb bag on a shelf (Task 2), removing a 1-gallon jug from a refrigerator (Task 6), brushing hair (Task 8), and opening a door with a latch handle (Task 10). These tasks primarily rely on power grasp configurations and benefit from the adaptive hand structure with whiffletree differentials. Moderate performance was observed in tasks requiring in-hand manipulation or precision actions. For example, opening a jug and pouring (Task 7) achieved an 80% success rate. Failures were primarily associated with in-hand manipulation skills of opening the jug lid. Similarly, using a fork (Task 9) achieved a 70% success rate. In these trials, incomplete closure of the hand limited cylindrical enclosure of the fork handle, occasionally resulting in object slippage. Two tasks were completely unsuccessful across all trials. Opening a sealed water bottle (Task 3) revealed insufficient transmitted torque to break the bottle cap seal. In particular, the prosthesis was able to reach, grasp, and stabilize the bottle, but the current pinch force is not sufficient to break the seal. Removing a wallet from a pocket (Task 4) proved challenging due to the constrained workspace and the lack of independent finger motion required for fine manipulation of the hand in confined spaces. Insufficient grasping force is due to a number of factors, such as inefficiencies in finger routing and a flexible harness material that reduced maximum force transmission.

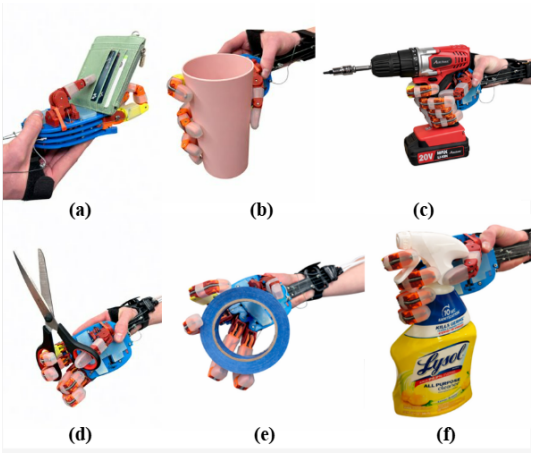

Fig. 9. Grasping of everyday objects: (a) Wallet; (b) Cup; (c) Cordless drill; (d) Pair of scissors; (e) Roll of tape; and (f) Spray bottle.

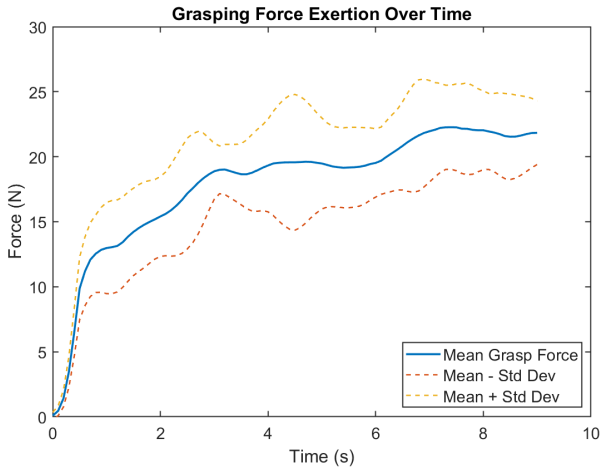

Fig. 10. Mean grasping force profile with ± 1 standard deviation across ten power grasp trials. Peak mean force of 22.3 N was achieved at approximately $t = 7.5$ s, with a maximum single-trial force of 25.6 N.

D. Everyday Object Grasp Evaluation

To further evaluate functional versatility beyond standardized assessment metrics, the prosthetic hand was tested on a range of common household objects varying in size, geometry, and weight. These included cylindrical objects (cup, spray bottle), flat objects (wallet), tools (cordless drill, scissors), and irregular shapes (roll of tape). As shown in Fig. 9, the body-powered prosthesis executes stable power grasps for heavier and larger objects, including the cordless drill and spray bottle, highlighting effective force transmission through the underactuated differential system. Although resetting modes requires cycling through all modes that must be reset, in practical use a single grasping posture with thumb fully opposing the fingers and the four fingers slightly adducted was found to be a natural pose that was effective for many tested objects, meaning that the F/E mode was the primary mode engaged and frequent mode switching was not necessary. It should also be noted that mode switching can be performed while the hand is loaded, allowing the user to achieve a grasp and then change modes to neutral while maintaining the grasp. Similarly to the BAM-ULA test, limitations are observed during in-hand manipulation tasks that require high precision and fingertip control. The system excels at grasping objects from a preset adduction and thumb opposition setting, but in-hand manipulation is challenging as multiple modes cannot be engaged simultaneously, and many in-hand manipulation tasks require concurrent execution of F/E and Ad/Ab.

E. Grasping Force Assessment

Grasping force of the hand is evaluated through bench testing across 10 repeated power grasp trials to assess force transmission consistency and magnitude with the body-powered prosthesis. Force is measured using the Vernier Hand Dynamometer, positioned at the fingertip contact surface, and data were recorded at 0.1 s intervals. Fig. 10 presents the mean grasping force profile with ± 1 standard deviation bounds across all trials. The prosthetic hand achieved a peak mean grasping force of 22.3 N, with an overall maximum recorded force at 25.6 N. The sustained mean force during the hold phase (approximately $t = 4$ s to $t = 9$ s) remained stable at 20–23 N, indicating consistent force transmission through the whiffletree differential and Bowden cable routing. The results reveal that the proposed body-powered prosthesis delivers sufficient grasping force for the majority of tasks evaluated in the BAM-ULA protocol while maintaining consistent and repeatable force transmission.

V. Conclusion

This paper presents an open-source body-powered prosthetic system that integrates an underactuated anthropomorphic hand with a selective gear-based clutch mechanism for switching between functional modes using a single input cable. The proposed transmission mechanically routes actuation to different tendon pathways, enabling flexion/extension of all fingers, adduction/abduction of the four fingers, and thumb opposition while locking inactive modes. Experimental results, including the BAM-ULA assessment and grasping demonstrations with everyday objects, show that the prosthesis reliably performs a wide range of daily tasks, achieving stable power grasps and consistent force transmission while maintaining the simplicity and affordability of body-powered devices. At the same time, the experiments reveal limitations associated with the sequential nature of the functional modes. Because the modes cannot be actuated simultaneously, tasks that require complex in-hand manipulation or coordinated multi-degree-of-freedom finger motion remain challenging. Overall, the results demonstrate that purely mechanical mode-switching mechanisms expand the capabilities of body-powered prostheses while preserving their core advantages of simplicity and affordability.

Clutch-specific metrics such as switching time, locking torque, and cyclic durability were not characterized in this work and are the focus of ongoing work. In addition, we are focusing on improving the cable routing system to reduce friction losses and increase grasp force.

REFERENCES

[1] N. A. Hashim, N. A. Abd Razak, N. A. Abu Osman, and H. Gholizadeh, "Improvement on upper limb body-powered prostheses (1921–2016): A systematic review," *Proceedings of the Institution of Mechanical Engineers, Part H: Journal of Engineering in Medicine*, vol. 232, no. 1, pp. 3–11, 2018.

[2] S. M. Engdahl, M. A. Gonzalez, C. Lee, and D. H. Gates, "Perspectives on the comparative benefits of body-powered and myoelectric upper limb prostheses," *Journal of NeuroEngineering and Rehabilitation*, vol. 21, no. 1, p. 138, 2024.

[3] J. T. Belter, J. L. Segil, A. M. Dollar, and R. F. Weir, "Mechanical design and performance specifications of anthropomorphic prosthetic hands: A review," *Journal of Rehabilitation Research and Development*, vol. 50, no. 5, p. 599, 2013.

[4] D. Plettenburg, "Upper limb prostheses-future perspectives for body-powered prostheses," in *Myoelectric Controls Symposium*, 2022.

[5] A. M. Dollar and R. D. Howe, "The highly adaptive SDM hand: Design and performance evaluation," *The International Journal of Robotics Research*, vol. 29, no. 5, pp. 585–597, 2010.

[6] J. T. Belter and A. M. Dollar, "Novel differential mechanism enabling two DOF from a single actuator: Application to a prosthetic hand," in *IEEE Inter. Conference on Rehabilitation Robotics*, pp. 1–6, 2013.

[7] G. P. Kontoudis, M. V. Liarokapis, A. G. Zisimatos, C. I. Mavrogiannis, and K. J. Kyriakopoulos, "Open-source, anthropomorphic, underactuated robot hands with a selectively lockable differential mechanism: Towards affordable prostheses," in *IEEE/RSJ International Conference on Intelligent Robots and Systems*, pp. 5857–5862, 2015.

[8] G. Gao, A. Dwivedi, and M. Liarokapis, "An anthropomorphic prosthetic hand with an active, selectively lockable differential mechanism: Towards affordable dexterity," in *IEEE/RSJ International Conference on Intelligent Robots and Systems*, pp. 6147–6152, 2021.

[9] G. Gao, M. Shahmohammadi, L. Gerez, G. Kontoudis, and M. Liarokapis, "On differential mechanisms for underactuated, lightweight, adaptive prosthetic hands," *Frontiers in Neurorobotics*, vol. 15, p. 702031, 2021.

[10] M. G. Catalano, G. Grioli, E. Farnioli, A. Serio, C. Piazza, and A. Bicchi, "Adaptive synergies for the design and control of the Pisa/IIT SoftHand," *The International Journal of Robotics Research*, vol. 33, no. 5, pp. 768–782, 2014.

[11] C. Piazza, G. Grioli, M. G. Catalano, and A. Bicchi, "A century of robotic hands," *Annual Review of Control, Robotics, and Autonomous Systems*, vol. 2, no. 1, pp. 1–32, 2019.

[12] G. McGimpsey and T. C. Bradford, "Limb prosthetics services and devices," *Bioengineering Institute Center for Neuroprosthetics Worcester Polytechnic Institution*, pp. 1–35, 2008.

[13] D. Segura, E. Romero, V. E. Abarca, and D. A. Elias, "Upper limb prostheses by the level of amputation: A systematic review," *Prosthesis*, vol. 6, no. 2, pp. 277–300, 2024.

[14] R. Brack and E. H. Amalu, "A review of technology, materials and R&D challenges of upper limb prosthesis for improved user suitability," *Journal of Orthopaedics*, vol. 23, pp. 88–96, 2021.

[15] H. de Visser and J. L. Herder, "Force-directed design of a voluntary closing hand prosthesis," *Journal of Rehabilitation Research and Development*, vol. 37, no. 3, pp. 261–272, 2000.

[16] M. E. Abbott, A. I. McPherson, W. O. Torres, K. Adachi, and H. S. Stuart, "Effect of variable transmission on body-powered prosthetic grasping," in *Inter. Conf. on Rehabilitation Robotics*, pp. 1–6, 2022.

[17] A. I. McPherson, M. E. Abbott, W. White, Y. Gloumakov, and H. S. Stuart, "A wearable testbed for studying variable transmission in body-powered prosthetic gripping," in *International Conference on Rehabilitation Robotics*, pp. 1–6, 2023.

[18] L. Birglen, T. Laliberté, and C. M. Gosselin, *Underactuated robotic hands*, vol. 40. Springer, 2007.

[19] M. Baril, T. Laliberté, C. Gosselin, and F. Routhier, "On the design of a mechanically programmable underactuated anthropomorphic prosthetic gripper," *Journal of Mechanical Design*, vol. 135, no. 12, p. 121008, 2013.

[20] A. Grazioso, D. C. Potenza, G. A. Zappatore, and G. Reina, "Performance analysis of the underactuated finger for Adam's hand," *IEEE Access*, vol. 12, pp. 149492–149501, 2024.

[21] G. Li, X. Liang, Y. Gao, T. Su, Z. Liu, and Z.-G. Hou, "A linkage-driven underactuated robotic hand for adaptive grasping and in-hand manipulation," *IEEE Transactions on Automation Science and Engineering*, vol. 21, no. 3, pp. 3039–3051, 2023.

[22] B. Busby, G. Gao, and M. Liarokapis, "An adaptive, lightweight, body-powered system for prosthetic hands equipped with a selectively lockable differential mechanism," in *International Conference of the IEEE Engineering in Medicine & Biology Society*, pp. 1–7, 2023.

[23] H. C. Lee and R. Cipra, "Design of a novel locking ratcheting mechanism for a body-powered underactuated hand," *Journal of Medical Devices*, vol. 14, no. 1, p. 011101, 2020.

[24] M. Santello, M. Flanders, and J. F. Soechting, "Postural hand synergies for tool use," *Journal of Neuroscience*, vol. 18, no. 23, pp. 10105–10115, 1998.

[25] I. Llop-Harillo, A. Pérez-González, and J. Andrés-Esperanza, "Grasping ability and motion synergies in affordable tendon-driven prosthetic hands controlled by able-bodied subjects," *Frontiers in Neurorobotics*, vol. 14, p. 57, 2020.

[26] E. Todorov and Z. Ghahramani, "Analysis of the synergies underlying complex hand manipulation," in *Inter. Conf. of the IEEE Engineering in Medicine and Biology Society*, vol. 2, pp. 4637–4640, 2004.

[27] C. Della Santina, M. Bianchi, G. Averta, S. Ciotti, V. Arapi, S. Fani, E. Battaglia, M. G. Catalano, M. Santello, and A. Bicchi, "Postural hand synergies during environmental constraint exploitation," *Frontiers in Neurorobotics*, vol. 11, p. 41, 2017.

[28] C. Della Santina, C. Piazza, G. Grioli, M. G. Catalano, and A. Bicchi, "Toward dexterous manipulation with augmented adaptive synergies: The Pisa/IIT SoftHand 2," *IEEE Transactions on Robotics*, vol. 34, no. 5, pp. 1141–1156, 2018.

[29] G. P. Kontoudis, M. Liarokapis, and K. G. Vamvoudakis, "An adaptive, humanlike robot hand with selective interdigitation: Towards robust grasping and dexterous, in-hand manipulation," in *IEEE-RAS International Conference on Humanoid Robots*, pp. 251–258, 2019.

[30] H. Yang, G. Wei, L. Ren, Z. Qian, K. Wang, H. Xiu, and W. Liang, "A low-cost linkage-spring-tendon-integrated compliant anthropomorphic robotic hand: MCR-Hand III," *Mechanism and Machine Theory*, vol. 158, p. 104210, 2021.

[31] G. Gao, J. Chapman, S. Matsunaga, T. Mariyama, B. MacDonald, and M. Liarokapis, "A dexterous, reconfigurable, adaptive robot hand combining anthropomorphic and interdigitated configurations," in *IEEE/RSJ International Conference on Intelligent Robots and Systems*, pp. 7209–7215, 2021.

[32] B. Buchholz, T. J. Armstrong, and S. A. Goldstein, "Anthropometric data for describing the kinematics of the human hand," *Ergonomics*, vol. 35, no. 3, pp. 261–273, 1992.

[33] G. P. Kontoudis, M. Liarokapis, K. G. Vamvoudakis, and T. Furukawa, "An adaptive actuation mechanism for anthropomorphic robot hands," *Frontiers in Robotics and AI*, vol. 6, p. 47, 2019.

[34] V. K. Nanayakkara, G. Cotugno, N. Vitzilaios, D. Venetsanos, T. Nanayakkara, and M. N. Sahinkaya, "The role of morphology of the thumb in anthropomorphic grasping: A review," *Frontiers in Mechanical Engineering*, vol. 3, p. 5, 2017.

[35] G. P. Kontoudis, M. Liarokapis, and K. G. Vamvoudakis, "A compliant, underactuated finger for anthropomorphic hands," in *IEEE International Conference on Rehabilitation Robotics*, pp. 682–688, IEEE, 2019.

[36] J. E. Shigley, R. G. Budynas, and J. K. Nisbett, *Shigley's mechanical engineering design*, vol. 8. McGraw Hill, 2008.

[37] V. V. Patel, M. V. Liarokapis, and A. M. Dollar, "Open robot hardware: Progress, benefits, challenges, and best practices," *IEEE Robotics & Automation Magazine*, vol. 30, no. 3, pp. 123–148, 2022.

[38] R. R. Ma, J. T. Belter, and A. M. Dollar, "Hybrid deposition manufacturing: Design strategies for multimaterial mechanisms via three-dimensional printing and material deposition," *Journal of Mechanisms and Robotics*, vol. 7, no. 2, p. 021002, 2015.

[39] M. V. Liarokapis, P. K. Artemiadis, and K. J. Kyriakopoulos, "Quantifying anthropomorphism of robot hands," in *IEEE International Conference on Robotics and Automation*, pp. 2041–2046, 2013.

[40] A. Kapandji, "Clinical test of apposition and counter-apposition of the thumb," *Annales de chirurgie de la main: organe officiel des societes de chirurgie de la main*, vol. 5, no. 1, pp. 67–73, 1986.

[41] L. Resnik, M. Borgia, and F. Acluche, "Brief activity performance measure for upper limb amputees: BAM-ULA," *Prosthetics and Orthotics International*, vol. 42, no. 1, pp. 75–83, 2017.

[42] T. Feix, J. Romero, H.-B. Schmiedmayer, A. M. Dollar, and D. Kragic, "The grasp taxonomy of human grasp types," *IEEE Transactions on Human-Machine Systems*, vol. 46, no. 1, pp. 66–77, 2015.